

Westbrook's Molecular Gun: Discovery of Near-IR Micro-Structures in AFGL 618¹

Toshiya Ueta, David Fong, and Margaret Meixner

*Department of Astronomy, MC-221, University of Illinois at Urbana-Champaign, Urbana, IL 61801
 ueta@astro.uiuc.edu, d-fong@astro.uiuc.edu, meixner@astro.uiuc.edu*

ABSTRACT

We present high-sensitivity near-IR images of a carbon-rich proto-planetary nebula, AFGL 618, obtained with the Subaru Telescope. These images have revealed “bullets” and “horns” extending farther out from the edges of the previously known bipolar lobes. The spatial coincidence between these near-IR micro-structures and the optical collimated outflow structure, together with the detection of shock-excited, forbidden IR lines of atomic species, strongly suggests that these bullets and horns represent the locations from which [Fe II] IR lines arise. We have also discovered CO clumps moving at $> 200 \text{ km s}^{-1}$ at the positions of the near-IR bullets by re-analyzing the existing $^{12}\text{CO } J = 1 - 0$ interferometry data. These findings indicate that the near-IR micro-structures represent the positions of shocked surfaces at which fast-moving molecular clumps interface with the ambient circumstellar shell.

Subject headings: circumstellar matter — dust, extinction — infrared: stars — stars: mass loss — stars: individual (AFGL 618, CRL 618, IRAS 04395+3601)

1. Introduction

AFGL 618 (CRL 618, *IRAS* 04395+3601) is a carbon-rich, extremely evolved proto-planetary nebula (PPN) transforming itself into a planetary nebula (PN). Since its identification (Westbrook et al. 1975), AFGL 618 has been extensively studied as one of the prime examples of a bipolar PPN (e.g., Carsenty & Solf 1982; Latter et al. 1992). From early observations, the emission from the bipolar lobes has been known to have two components: scattered star light through the biconical openings of an optically thick dust torus around the central star and shock-excited line emission arising from the lobes themselves (Schmidt & Cohen 1981; Kelly, Latter, & Rieke 1992).

Recent Hubble Space Telescope (*HST*) observations in shock-excited line emission have revealed collimated outflow structure in the bipolar lobes (Trammell 2000). This evident connection be-

tween the bipolar morphology and the collimated outflows suggests the presence of very effective collimation mechanism(s) at work in the innermost region of AFGL 618, possibly deep within the dust torus. Here we present results from high-resolution, high-sensitivity near-IR imaging of AFGL 618 using the 8.2 m Subaru Telescope and discuss their implications.

2. Observations

We observed AFGL 618 using the Infrared Camera and Spectrograph (IRCS; Kobayashi et al. 2000) at the Subaru Telescope on 2001 February 5 (Program ID: S00-072). The IRCS has two Raytheon ALADDIN II InSb arrays, which give $60'' \times 60''$ field of view at $0''.058 \text{ pix}^{-1}$ without adaptive optics. The observations were made under marginally clear but very gusty conditions. Seeing varied between $0''.6$ and $0''.9$ throughout the night. We employed an on-chip, 5-point dithered pattern to image and used long exposure times to detect faint nebulosities. Table 1 summarizes the observations.

¹Based partially on data obtained at the Subaru Telescope, which is operated by the National Astronomical Observatory of Japan.

Standard IR data reduction and calibration procedures were followed, except that the images were extinction-corrected using the averaged correction factors for Mauna Kea (Krisciunas et al. 1987) because the correction factors were not reliably derived from the data. In addition, continuum emission in the H_2 and $Br\gamma$ images was subtracted by estimating continuum emission at these bands from the K -continuum image. Absolute flux calibration errors are estimated to be approximately $\pm 10\%$, which reflects the less-than-average sky conditions. While our K' magnitude is comparable to the K magnitude of Westbrook et al. (1975) despite the recent reports on the increase of the integrated flux at K (Latter et al. 1992, 1995), our J and H magnitudes are brighter than previously measured. The change in the brightness could be intrinsic to the rapidly evolving nature of the object, however, the quality of our data prevents us from elaborating further.

Selected near-IR images of AFGL 618 are presented in Fig. 1. In these images, any small variations of the surface brightness were obscured by very strong emission from the central peak. Thus, we applied unsharp masks to the original images to enhance small variations in surface brightness. Such structure-enhanced images, presented alongside the original images, have successfully revealed the clumpy structure of the nebula.

3. Results and Discussions

3.1. Deep Near-IR Images

The near-IR emission structure of AFGL 618 consists of a highly centralized peak and a faint nebulosity that is elongated in the E-W direction. The J band image clearly shows the bipolarity of the source as seen in the optical (e.g., Westbrook et al. 1975). A similar E-W elongation is seen at H (not shown). The K' band image is relatively wider in the N-S direction compared with the images at J and H . A similar morphological trend has been seen previously and model calculations have suggested that dust scattering would be the primary source of the morphological change in the near-IR (Latter et al. 1992). The overall emission structure of the nebula is such that the eastern lobe is significantly brighter than the western lobe due to the central peak located in the eastern lobe. This corroborates our current understanding

of the structure of AFGL 618, in which a bipolar nebula with a wide opening angle is inclined at $\sim 45^\circ$ with respect to the line of sight with its eastern lobe pointing towards us (e.g., Carsenty & Solf 1982).

In addition to the previously known bipolar lobes, we have detected three “bullets” that are isolated from the western lobe by about $2''$ and two “horns” that are connected to the eastern lobe. Our images present the first clear detection of these micro-structures owing to better resolution and sensitivities. Previous near-IR images (Latter et al. 1992) seem to show some evidence for the eastern horns in the noisy lowest contours, but did not cover the region of the sky in which the western bullets are present. The most recent images by Latter et al. (1995), while failing to show the eastern horns due to the coarse pixel scale ($0''.6\text{ pix}^{-1}$), appear to indicate that there is a region of extended emission spatially coincident with the brightest western bullet. Although the extension seems to be isolated from the western lobe, it was not recognized as a micro-structure. In the present image at J , the brightness of the two brighter bullets are at least comparable to the peak of the western lobe. In the most recent J image (Latter et al. 1995), however, the tip of the western extension appeared to be dimmer than the western lobe and the middle bullet was not even seen. Thus, these bullets may be varying their brightnesses and/or positions (see §3.3) in the past years. Therefore, continued monitoring of these micro-structures will be worthwhile.

The continuum-subtracted narrowband images also show a similar elongation in a somewhat different manner. In H_2 , the central peak is less prominent and, while the eastern horns can be slightly visible, there is no apparent western bullets. Although the H_2 emission is known to have both thermally excited and UV fluorescent components (Latter et al. 1992), our image alone can not isolate these components. There appear to be faint protrusions emanating from the central peak at the $3\sigma_{\text{sky}}$ level, along the equatorial plane defined by the “dust waist.” These equatorial structures may be similar to those seen in another well-known PPN, AFGL 2688 (the Egg Nebula, Sahai et al. 1998). On the other hand, the $Br\gamma$ image, which originates from the compact H II region around the central star (Kwok & Bignell 1984),

is very compact.

Meanwhile, there is a growing interest on a particular type of morphology, so-called “concentric arcs,” which are typically found around evolved stars (e.g., Hrivnak, Kwok, & Su 2001). These arcs appear to be limb-brightened segments of spherical shells created by the asymptotic giant branch (AGB) wind. The apparent coexistence of concentric arcs within a bipolar nebula as seen, for example, in AFGL 2688 (Sahai et al. 1998) presents a challenge in formulating a mass loss scenario in evolved stars. Despite the new discoveries of the bullets and horns, we do not find any apparent evidence for the presence of the concentric arcs in our images above one σ_{sky} level.

3.2. Near-IR “Bullets” and “Horns”

The surface brightness of the bullets and horns is comparable: the brightest western bullet in J is actually the second brightest point in the entire nebulosity. This emission structure is unusual because the surface brightness due to scattered stellar emission is expected to decrease monotonically as the distance from the central star increases. In such a case, the western (far) side of the nebula should appear darker than the eastern (near) side.

In fact, the bullets and horns are spatially coincident with the tips of the collimated outflows imaged in shock-excited forbidden lines ($[\text{O I}]$ 6300Å and $[\text{S II}]$ 6717, 6731Å) by *HST* (Trammell 2000). The emission clumps seen throughout the nebula in the structure-enhanced images agree quite well with the optical outflow morphology in the *HST* images. Moreover, Kelly, Latter, & Rieke (1992) detected $[\text{Fe II}]$ lines at 1.321 & 1.328 μm at 4 to 6'' east and 4'' west of the mid-point between the optical bipolar lobes. These locations respectively coincide with the positions of the horns and bullets. Hora, Latter, & Deutsch (1999) have, in addition, detected relatively strong $[\text{Fe II}]$ lines at 1.26 and 1.64 μm from this object. Since $[\text{Fe II}]$ IR lines are known to be good probes of jets and shocks in dense material (e.g., Graham, Wright, & Longmore 1987; Reipurth et al. 2000), we would conclude that the newly detected near-IR bullets and horns are mainly caused by *in situ* shock-excited $[\text{Fe II}]$ line emission.

This interpretation would not conflict with the unusual emission structure within the nebula be-

cause the strength of the line emission depends on the shock conditions and geometry. The difference in the micro-structures (bullets vs. horns) can be attributed to the different degree of collimation of the outflows in the lobes. The *HST* images show a narrower outflow structure in the western lobe than in the eastern lobe. This may imply that the shock surfaces are distributed over a larger area in the eastern lobe than in the western lobe, resulting in equally bright horns and bullets despite the presumed inclination of the bipolar nebula. While the brightest southernmost bullet is barely visible, the middle bullet is the brightest in $[\text{S II}]$ and $[\text{O I}]$ (Trammell 2000). This can also be attributed to different excitation conditions among these bullets. Future high-resolution spectroscopy would be needed to determine shock conditions in these micro-structures.

While the bullets seem to be a unique feature among PPNs, the horns resemble the ones seen in AFGL 2668 Latter et al. (1995); Sahai et al. (1998). However, the origins of the horns do not seem to be the same. In the case of AFGL 618, the horns seem to be a result of outflows towards the polar region of the nebula, whereas the horns in AFGL 2668 is a result of scattering (Latter et al. 1995; Sahai et al. 1998). This indicates that different mechanisms could form similar morphologies and thus the nebula shaping mechanism may not be uniquely identified from the morphology alone.

3.3. Near-IR Bullets vs. Molecular Bullets

Trammell (2000) argued, based on the excitation gradient in the outflows, that the collimated morphology is a result of material flows impinging on the surrounding medium. In fact, AFGL 618 is known to host one of the fastest molecular outflows ever found in the Galaxy (e.g., Burton & Geballe 1986). Especially of interest are the single dish observations of CO (Cernicharo et al. 1989; Gammie et al. 1989), in which the authors have detected outflows at $> 200 \text{ km s}^{-1}$. The follow-up interferometric observations (Neri et al. 1992; Hajian, Phillips, & Terzian 1996), however, have detected only medium velocity ($\sim 70 \text{ km s}^{-1}$) outflows in the central region. While Kastner et al. (2001) have demonstrated that the high velocity ($\sim 120 \text{ km s}^{-1}$) H_2 tends to be found closest to the central star, their position-velocity map also shows

the presence of fast moving clumps near the edge of the bipolar nebulosity. In any case, CO outflows at $> 200 \text{ km s}^{-1}$ have not yet been spatially identified.

As we have seen, our near-IR images have revealed locations from which shock-excited [Fe II] line emission seems to arise, and therefore, these bullets and horns may well represent the shocked surfaces of high-velocity “CO bullets” which are penetrating into an ambient AGB shell. To obtain more kinematical insights, we have re-analyzed millimeter interferometry data of the ^{12}CO $J = 1 - 0$ line emission originally presented elsewhere (Meixner et al. 1998). In this analysis, we have used only the high-resolution data (UV range of $7 - 91\text{k}\lambda$) to spatially filter out the extended emission. Robust weighting of the visibility data yielded a $2''.0 \times 1''.7$ CLEAN beam with a position angle of 54.7° . This resolution is appropriate for direct comparisons with the near-IR images. Fig. 2 shows the false-color J band image overlaid with CO contours integrated between -140 km s^{-1} and 100 km s^{-1} . Also displayed are CO spectra obtained from a $2'' \times 2''$ patch of the sky at eight locations in the nebula. In these spectra, typical rms noise per 8 km s^{-1} channel is $0.07 \text{ Jy beam}^{-1}$.

The emission peak spectrum (panel D) shows both blue- and red-shifted wings on both sides of the broad peak at $\sim 21.5 \text{ km s}^{-1}$ representing the central velocity of the object (Neri et al. 1992; Hajian, Phillips, & Terzian 1996). A deep dip in the blue-shifted wing is due to self-absorption (Neri et al. 1992; Hajian, Phillips, & Terzian 1996; Meixner et al. 1998). The spectra of the lobes (C and E) respectively exhibit large blue- and red-shifted wings as expected from the presumed bipolar outflow. On the other hand, the spectra of the horns (A and B) seem to indicate the presence of faint broad wings on both sides of the peak at the central velocity. This large velocity dispersion is consistent structure-wise with the less-collimated eastern horns as suggested by the near-IR emission strengths and the optical outflow morphologies. The spectra of the bullets (F, G, and H) do not show any apparent red-shifted wings, but high-velocity “clumps” appear to be present. At the positions of the two brightest bullets (G and H), we detect emission from clumps moving at about -220 km s^{-1} . Although weak in absolute inten-

sity, emission from these clumps registers about 4σ in the position-velocity diagrams. In addition, velocity channel maps show consistent structures over several velocity frames around -220 km s^{-1} . Therefore, we conclude that the detections of these high-velocity CO clumps are real.

There also appear to be CO clumps moving at different velocities. For example, there are clumps moving at about -140 and -45 km s^{-1} respectively at F and H. The existence of an ensemble of fast moving clumps have already been observed in H_2 (Burton & Geballe 1986). This coincidence of the fast moving CO clumps and shock-excited IR and optical emission regions strongly suggests that shock excitation is induced as these molecular bullets impinge on the ambient medium.

This is the first spatial identification of the fastest moving components of CO emission in AFGL 618. Fast molecular outflows have been well studied in the context of Herbig-Haro (HH) objects. Herbst et al. (1996) observed jets in T Tau at [Fe II] $1.644 \mu\text{m}$ and H_2 $2.122 \mu\text{m}$ and attributed the spatial displacement between the peaks in these bands to the orientation of the jet head with respect to observers. In their scenario, [Fe II] line emission comes from the head of the outflow where dissociative, fast shock is induced and H_2 emission comes from the oblique bow-shocked zone that forms the “wakes” behind the advancing molecular bullets. Comparing our J and H_2 images (especially the structure-enhanced ones), we immediately see that H_2 emission structure outlines the periphery of the wakes behind the CO bullets (bullets and horns in J) as seen in the Orion nebula (Allen & Burton 1993). To secure the detection of high-velocity molecular clumps, we need to investigate kinematics of molecular species at not only the central part but also the edges of the bipolar structure.

4. Summary

We have discovered near-IR micro-structures (bullets and horns) extending farther out from the previously known bipolar structure of an evolved PPN, AFGL 618. Based on the emission structure of the micro-structures and the results from the previous spectroscopy, we have concluded that the near-IR micro-structures are likely due to line contamination by shock-excited IR lines, especially by

the [Fe II] lines. We have also found the fastest moving ($\sim 220 \text{ km s}^{-1}$) CO molecular clumps coincident with the positions of the near-IR micro-structures. These findings strongly suggest that shock-excitation is being induced by fast-moving CO clumps impacting on the surrounding medium at the positions of the micro-structures located at the edges of the bipolar nebula. The presence of HH type molecular flows is very likely, as suggested from the morphological relationship between shock-excited line emission (represented by near-IR bullets and horns) and H₂ emission. It will be worthwhile to continue observing AFGL 618 for its full spatial extent at the highest resolutions in the optical and near-IR to see if there really exist brightness and/or spatial variations and in molecular lines to better characterize the velocity structures and the shock geometry in evolved stars. Proper understanding of these molecular outflows and the resulting shocks is of critical importance for constructing the theory of structure formation at the earliest PN phase.

Ueta would like to thank the IRCS support scientist, Dr. Hiroshi Terada, and the staff at the Subaru Telescope for their support. An anonymous referee is thanked for valuable comments. We also acknowledge support from the NSF CAREER award AST 97-33697, the Laboratory for Astronomical Imaging at the University of Illinois, and NSF grant AST 99-81363.

REFERENCES

Allen, D. A., & Burton, M. G. 1993, *Nature*, 363, 54

Burton, M. G., & Geballe, T. R. 1986, *MNRAS*, 223, 13

Carsenty, U., & Solf, J. 1982, *A&A*, 106, 307

Cernicharo, J., Guélin, M., Martin-Pintado, J., Peñalver, J., & Mauersberger, R. 1989, *A&A*, 222, L1

Gammie, C. F., Knapp, G. R., Young, K., Phillips, T. G., & Falgarone, E. 1989, *ApJ*, 345, L87

Graham, J. R., Wright, G. S., & Longmore, J. 1987, *ApJ*, 313, 847

Hajian, A. R., Phillips, J. A., & Terzian, Y. 1996, *ApJ*, 467, 341

Herbst, T. M., Beckwith, S. V. W., Glindemann, A., Tacconi-Garman, L. E., Kroker, H., & Krabbe, A. 1996, *AJ*, 111, 2403

Hora, J. L., Latter, W. B., & Deutsch, L. K. 1999, *ApJS*, 124, 195

Hrivnak, B. J., Kwok, S., & Su, K. Y. L. 2001, *ApJ*, in press

Kastner, J. H., Weintraub, D. A., Gatley, I., & Henn, L. 2001, *ApJ*, 546, 279

Kelly, D. M., Latter, W. B., & Rieke, G. H. 1992, *ApJ*, 395, 174

Kobayashi, N., et al. 2000, *SPIE*, 4008, 1056

Krisciunas, K., et al. 1987, *PASP*, 99, 887

Kwok, S., & Bignall, R. C. 1984, *ApJ*, 276, 544

Latter, W. B., Maloney, P. R., Kelly, D. M., Black, J. H., Rieke, G. H., & Rieke, M. J. 1992, *ApJ*, 389, 347

Latter, W. B., Kelly, D. M., Hora, J. L., & Deutsch, L. K. 1995, *ApJS*, 100, 159

Meixner, M., Campbell, M. T., Welch, W. J., & Likkel, L. 1998, *ApJ*, 509, 392

Neri, R., García-Burillo, S., Guélin, M., Cernicharo, J., Guiloteau, S., & Lucas, R. 1992, *ApJ*, 262, 544

Reipurth, B., Yu, K. C., Heathcote, S., Bally, J., & Rodríguez, L. F. 2000, *AJ*, 120, 1449

Sahai, R., et al. 1998, *ApJ*, 493, 301

Schmidt, G. D., & Cohen, M. 1981, *ApJ*, 246, 444

Tedds, J. A., Brand, P. W. J. L., & Burton, M. G. 1999, *MNRAS*, 307, 337

Trammell, S. R. 2000, in *ASP Conf. Ser.* 199. *Asymmetrical Planetary Nebulae II: From Origins to Microstructures*, ed. J. H. Kastner, N. Soker, & S. A. Rappaport (San Francisco: ASP), 147

Westbrook, W. E., Willner, S. P., Merrill, K. M., Schmidt, M., Becklin, E. E., Neugebauer, G., & Wynn-Williams, C. G. 1975, *ApJ*, 202, 407

TABLE 1
SUMMARY OF SUBARU/IRCS OBSERVATIONS OF AFGL 618

| Band | Filter λ ($\delta\lambda$) [μm] | Exposure (sec) | Size ($'' \times ''$) | Flux (mJy) | Peak ($1\sigma_{\text{sky}}$) (mJy arcsec^{-2}) |
|-------------------|---|-------------------|----------------------------|---------------|--|
| J | 1.25 (0.16) | 600, 1000 | 17.0×6.7 | 13 | 3 (0.003) |
| H | 1.63 (0.30) | 160 | 15.8×6.7 | 75 | 44 (0.02) |
| K' | 2.12 (0.35) | 80 | 14.2×7.9 | 118 | 63 (0.03) |
| H ₂ | 2.122 (0.032) | 300 | 12.4×5.2 | 187 | 49 (0.2) |
| Br γ | 2.166 (0.032) | 150 | 8.7×5.5 | 49 | 11 (0.1) |
| K _{cont} | 2.280 (0.032) | 200 | 8.5×5.5 | 193 | 110 (0.1) |

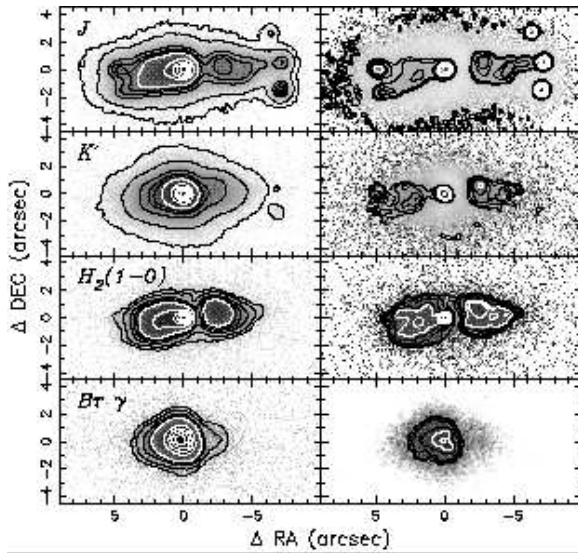


Fig. 1.— Selected near-IR images of AFGL 618 (left) and their structure-enhanced counterparts (right). The RA and DEC offsets are shown with respect to the peak. White contours run from 90% to 10% of the peak intensity with a 20% interval, then black contours are shown with an arbitrary spacing to outline the emission structure. The lowest contour represents $3\sigma_{\text{sky}}$. Contours seen well away from the bipolar lobes in the structure-enhanced images are artifacts in the image processing.

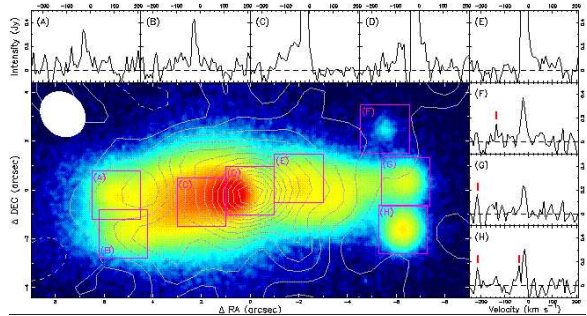


Fig. 2.— The false-color J image overlaid with the CO integrated map using the same convention as Fig. 1. The white ellipse at the top left indicates the beam shape. CO spectra at various positions are also displayed with negative values corresponding to blue-shifted velocities.